

HELSINKI UNIVERSITY OF  
TECHNOLOGY  
Laboratory of Physics

15th October 2006

Radiation damage in ion implanted and annealed  
*n*-type Ge studied by positron annihilation spectroscopy

M. Rummukainen  
J. Slotte  
F. Tuomisto  
V. P. Markevich  
A. R. Peaker

Helsinki University of Technology  
Publications in Engineering Physics  
Report TKK-F-A845 (2006)

# Chapter 1

## Introduction

In recent years we have witnessed a growing interest of germanium as an active element in semiconductor technology. The ever increasing performance demands, with decreasing feature sizes as a consequence, may better be met using germanium. Germanium allows for a higher channel mobility in MOSFET devices, for a extensive review of the use of germanium in MOSFET technology see Ref. [1]. Due to the dominance of silicon in semiconductor industry, very little research has been conducted on the basic properties of germanium, such as irradiation and implantation studies and point defects.

Positron annihilation spectroscopy (PAS) has been established as a versatile tool for studying open volume defects in semiconductors [2]. However, as with other techniques, very little work has been published on germanium. Positron lifetime studies have been performed on bulk crystals, with defects of monovacancy size reported by Moser *et al.* [3]. Vacancy clustering and the annealing of these clusters have been studied by Krause Rehberg *et al.* [4].

In this work we used positron annihilation spectroscopy (PAS) and Rutherford backscattering/channeling (RBS/C) to study lattice damage and defects created in the ion implantation of Ge and the annealing of the damage. Ge ions with 2 MeV energy and Si ions with 600 keV and 950 keV energy were used at implantation fluencies  $1 \times 10^{12} \text{ cm}^{-2}$  to  $4 \times 10^{14} \text{ cm}^{-2}$ . The Ge and Si fluencies were chosen to yield similar damage, as calculated by TRIM.

RBS/C revealed that the amorphization occurred in the samples implanted with the highest fluencies and already a fluence as low as  $1 \times 10^{13} \text{ cm}^{-2}$  results in 65-75 % of the atoms being displaced. An annealing temperature of 400 °C is required to recrystallize the samples. During recrystallization, a zipper band forms at a depth of roughly half of the projected ion range.

For the as-implanted samples PAS in the Doppler broadening mode give similar results for all fluencies. The measured  $S$  and  $W$  parameters indicate

that the average free volume in the track and projected range region is of divacancy size. After sample annealing we observe vacancy clustering and the cluster size depends on annealing temperature and ion fluence. Annealing at 500 °C was enough to remove all observable defects for ion fluencies below  $4 \times 10^{13} \text{ cm}^{-2}$ . For higher fluencies, some vacancy type defects are left in the samples.

# Chapter 2

## Experiment

### 2.1 Samples

We studied Si and Ge implanted *n*-type Ge samples. The samples were prepared from two Sb-doped Czochralski grown Ge wafers supplied by Umicore. The first wafer (samples 1x-x) was in the  $\langle 100 \rangle$  direction and the resistivity was measured to be  $\rho = 1.6 - 1.9 \text{ } \Omega\text{cm}$ . The orientation of the second wafer (samples 2x-x) was  $\langle 100 \rangle$  tilted  $9^\circ$  to wards  $\langle 111 \rangle$  with a resistivity  $\rho = 0.15 - 0.17 \text{ } \Omega\text{cm}$ .

Six sets of samples were implanted with Si and Ge at fluencies  $1 \times 10^{12}$  -  $4 \times 10^{14} \text{ cm}^{-2}$ . The ion energies were 600 keV and 950 keV for Si, and 2 MeV for Ge. The implantation depth corresponding to the 950 keV Si ions and 2 MeV Ge ions is approximately  $1 \text{ } \mu\text{m}$ . The samples were subsequently annealed for 30 min at temperatures 200, 300, 400 and  $500 \text{ } ^\circ\text{C}$  in an  $\text{N}_2$  atmosphere to study the defect evolution. The details of the samples can be found in Table 2.1. For the RBS/c study we chose a representative set from the samples used in the PAS study.

### 2.2 Experimental setup

Positron annihilation spectroscopy (PAS) is a useful tool for studying point defects. [2] The annihilation radiation can provide atomic resolution into defects and atoms surrounding them. Studies of defect distributions in thin layers or even defect profiling with the Doppler broadening technique are possible by controlling the implantation energy of the positrons.

We used a monoenergetic positron beam to study defects created by Si and Ge implantation in Ge. Positrons were obtained from a  $^{22}\text{Na}$  source and implanted into the samples at selected energies between 0.5 - 40 keV.

Table 2.1: Properties of the studied sample sets. Every set contains an as-implanted sample and samples annealed at 200, 300, 400 and 500 °C for 30 min.

Sample	Template	Ion	Energy	Fluence
11-x	Ge-1	Si	950 keV	$4 \times 10^{13} \text{ cm}^{-2}$
12-x	Ge-1	Ge	2 MeV	$1 \times 10^{13} \text{ cm}^{-2}$
13-x	Ge-1	Si	950 keV	$4 \times 10^{14} \text{ cm}^{-2}$
14-x	Ge-1	Ge	2 MeV	$1 \times 10^{14} \text{ cm}^{-2}$
21-x	Ge-2	Si	600 keV	$1 \times 10^{12} \text{ cm}^{-2}$
22-x	Ge-2	Ge	2 MeV	$1 \times 10^{13} \text{ cm}^{-2}$

The mean implantation depth of 40 keV positrons into Ge is approximately 2  $\mu\text{m}$ . After implantation positrons thermalize and diffuse in the lattice until annihilation. The positron diffusion length before annihilation varies from several hundred nanometers to less than ten nanometers depending on the types of defects and their concentration in the material. [2] Due to the missing positively charged nucleus the diffusing positrons can effectively be trapped by open volume defects, such as vacancies and vacancy clusters,

In Doppler broadening spectroscopy the momentum of the annihilating electron-positron pair is detected as broadening of the 511 keV annihilation peak. We used two Ge detectors with an energy resolution 1.3 eV at 511 keV for measuring the annihilation spectra. Two detectors can be used independently to achieve a double count rate. The annihilation spectrum were described using the conventional  $S$  and  $W$  shape parameters [5]. The  $S$  parameter describes the fraction of counts in the central region of the annihilation peak where the annihilating electron-positron pair momentum is low. These annihilations correspond mainly to valence electrons. The  $W$  parameter describes the fraction of annihilations in the wing regions on both sides of the annihilation spectrum. These annihilations are mostly with core electrons. The used  $S$  parameter energy window was  $p_\gamma < 3.2 \times 10^{-3} m_0c$ , where  $p_\gamma$  is the momentum of the electron-positron pair. The  $W$  parameter windows were selected as  $12 \times 10^{-3} m_0c < p_\gamma < 30 \times 10^{-3} m_0c$ .

The shape parameters reflect the environment of the annihilation site. Typically vacancies are detected as an increase (decrease) of the  $S$  ( $W$ ) parameter from the bulk value. For clusters of a few missing atoms the  $S$  parameter increases almost linearly with the vacancy size in Si. [6] The  $W$  parameter decreases at the same time but the decrease becomes smaller for every missing atom. For large vacancy clusters, however, both parameters

saturate. The measured  $S$  and  $W$  parameters are superpositions of  $S$  and  $W$  parameters corresponding to different positron annihilation states in the lattice.

For the RBS/channeling analysis we used a  ${}^4\text{He}^+$  1.554 MeV ion beam at scattering angles  $148.2^\circ$  and  $172.8^\circ$ . Channeling measurements were done with the beam aligned along the  $\langle 100 \rangle$  channel and with a beam current of approximately 10 nA.

# Chapter 3

## Experimental results

### 3.1 Rutherford backscattering/Channeling

Normalized RBS yield with beam aligned in the  $\langle 100 \rangle$  direction was measured for the as-implanted samples. The spectrum from sample implanted  $1 \times 10^{14} \text{ cm}^{-2}$  Ge ions coincides with the random spectrum, indicating that the sample is completely amorphous in the studied depth interval. Reducing the implantation fluence by a order of magnitude results in approximately 65 - 75 % of the atoms beeing displaced.

The annealing effects on the RBS/C yield from the set with Ge implantation fluence  $1 \times 10^{14} \text{ cm}^{-2}$  were studied. After annealing at 300 °C a 50 nm thin crystalline layer was formed at the surface. The 400 ° anneal essentially regrows the crystalline structure of the material, but leaves a large number of dislocations, together with a zipper defect band at 500 nm. The sample annealed at 500 °C seems to yield slightly more dechanneled ions than the sample annealed at 400 °C.

### 3.2 Positron annihilation spectroscopy

#### 3.2.1 Implantation damage

The ion implantation damage in the samples was studied by measuring the PAS spectra as a function of the positron implantation energy. Figure 3.1 shows the  $S$  parameter versus the positron implantation energy in the implanted samples and in the unimplanted Ge wafers for fluencies below  $1 \times 10^{14} \text{ cm}^{-2}$ . The data has been scaled to the parameters measured in bulk Ge giving  $S_{\text{Ge}}=0.517$  and  $W_{\text{Ge}}=0.036$ . In all the samples the  $S$  parameter strongly decreases at energies below 5 keV due to positron diffusion and annihilations

at the sample surface. As the positron implantation energy is increased the  $S$  parameter in the implanted samples increases to  $S=1.047$  until at the highest energies,  $E > 20$  keV, the  $S$  parameter starts to decrease. The decrease of the  $S$  parameter at high positron implantation energies is expected as positrons penetrate deeper than the implanted ions thus probing the defect free Ge wafer. The unimplanted samples show a long positron diffusion length and an identical depth profile as the bulk Ge reference indicating the defect concentration is below the PAS detection limit,  $< 10^{15} \text{ cm}^{-3}$ .

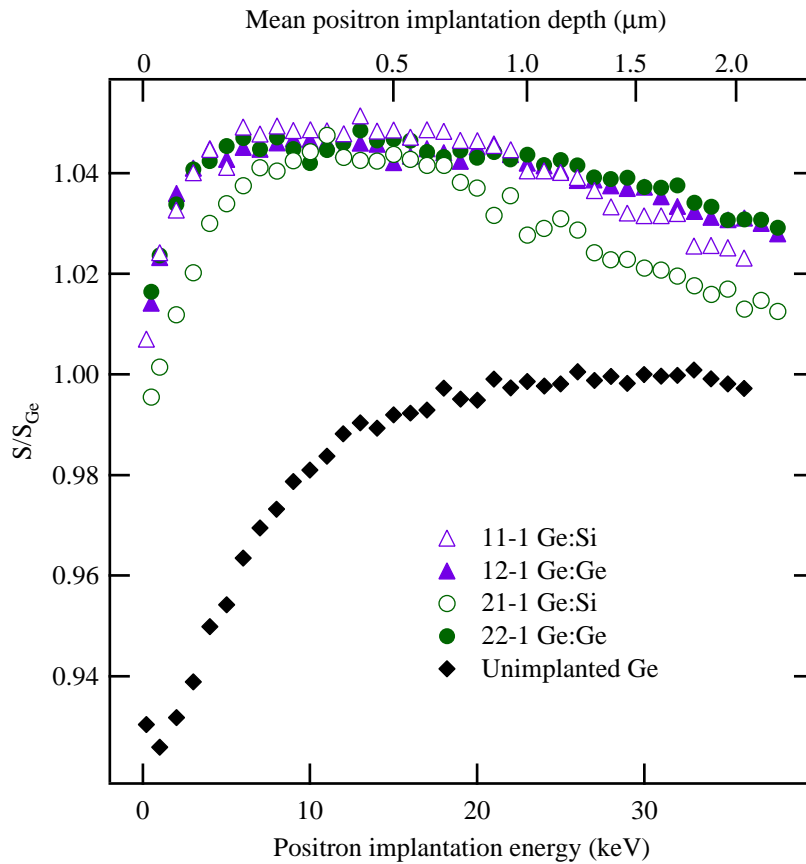


Figure 3.1: The low momentum  $S$  parameter in the as-implanted samples. The data has been scaled to the parameters measured in bulk Ge with  $S_{\text{Ge}}=0.517$ . The mean positron implantation depth is shown on the top axis.

The  $S$  parameter curve for the samples with the implantation fluence over  $1 \times 10^{13} \text{ cm}^{-3}$  (all samples except 21-1) is flat between 5 keV and 20 keV. The level of the  $S$  parameter does not depend on the fluence or the ion.



This shows the same type of defects are present and the concentration of positron trapping defects is high enough to produce saturated trapping into open volume defects. Similar saturation of the annihilation parameters after ion implantation has been found earlier in Si [7]. Ion irradiation generates vacancies and interstitials, which are mobile at the implantation temperature. [8] The migrating vacancies can form stable complexes with the Sb dopant atoms or other vacancies. [9] The  $S$  parameter curve of the sample 21-1 with the lowest studied fluence is smooth but peaks at the level observed in the other layers. This suggests that the defects with similar open volume are formed but at a lower concentration.

### 3.2.2 Annealing effects

The implanted layers were annealed at 200 - 500 °C for 30 min to study the temperature evolution of the defects created. The measured curves for the  $S$  parameter in the sample with Ge fluence  $1 \times 10^{13} \text{ cm}^{-3}$  for different annealing temperatures are shown in Fig. 3.2. In all the layers we observe the surface at low positron implantation energies and the unimplanted wafer at  $E > 20 \text{ keV}$ . At energies 5 - 20 keV there is a peak in the  $S$  parameter that corresponds to defects in the implanted layer. The height of the peak increases for annealings up to 400 °C, while after annealing at 500 °C the measured  $S$  parameter is close to that observed in the bulk Ge.

Vacancy-donor pairs and divacancies have been found to be mobile in Ge already at the lowest annealing temperature 200 °C. [10, 8, 9] After annealing at 200 °C the  $S$  parameter forms a peak at  $S \approx 1.09$ , more than twice the value recorded in the as-implanted value. At the same time there is a corresponding decrease in the  $W$  parameter. The  $S$  parameter is closely related to the open volume of the defects and the observations suggest that the vacancies observed after 200 °C anneal have more than twice the open volume of the defects in the as-implanted sample.

Annealing the samples to 300 °C the  $S$  parameter increases to  $S \approx 1.10$  and a further anneal at 400 °C increases the  $S$  parameter to  $S \approx 1.11$ . The further increase of the  $S$  parameter after anneals at 300 and 400 °C suggests that the size of the vacancy clusters increases. Finally, the  $S$  parameter drops to approximately the level observed in the bulk Ge after an anneal at 500 °C. This shows that most defects anneal out of the sample at 500 °C. This is consistent with earlier studies on annealing of ion implantation damage and recrystallization of amorphous Ge where it has been found that the defects are removed at temperatures 300 - 500 °C. [11, 12, 13] The annealing temperature of the observed vacancy clusters is similar to what Krause-Rehberg *et al.* [4] found in high-stress and low-temperature deformed high purity germanium.

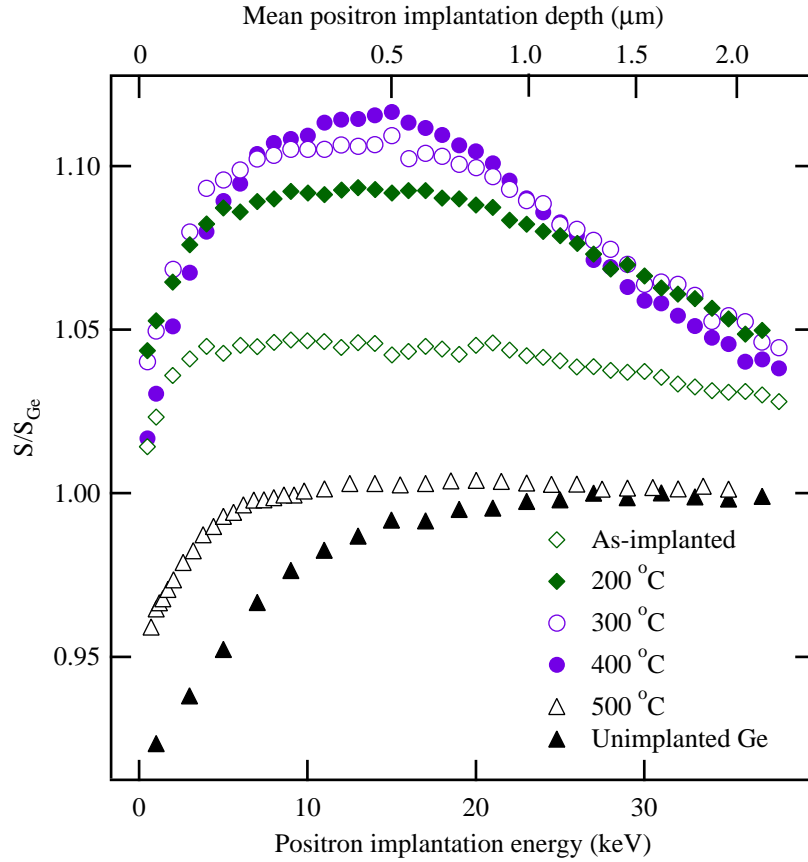


Figure 3.2: The low momentum  $S$  parameter measured at room temperature after 30 min anneal for the set 12-x with Ge fluence  $1 \times 10^{13} \text{ cm}^{-2}$ . The data has been scaled to the parameters measured in bulk Ge with  $S_{Ge}=0.517$ .

Vacancy clustering was observed also in the set 21-x, where the Si implantation fluence was  $1 \times 10^{12} \text{ cm}^{-3}$ . The  $S$  parameter curves for different annealing temperatures are shown in Fig. 3.3. The  $S$  parameter increases in the anneal at 200 °C but remains below that observed in the other sample sets. The lower  $S$  parameter can be due to a smaller cluster size or a lower cluster concentration. This is expected when the clusters form through conglomeration of smaller mobile defects and the original defect concentration is lower. After annealing at 300 °C the  $S$  parameter is slightly below the level observed after 200 °C anneal. Annealing the sample at 400 °C the  $S$  parameter drops to a level  $S=1.007$ , indicating nearly all the defects were removed in the anneal. The  $S$  parameter decreases further after an anneal at 500 °C and no defects are detected.

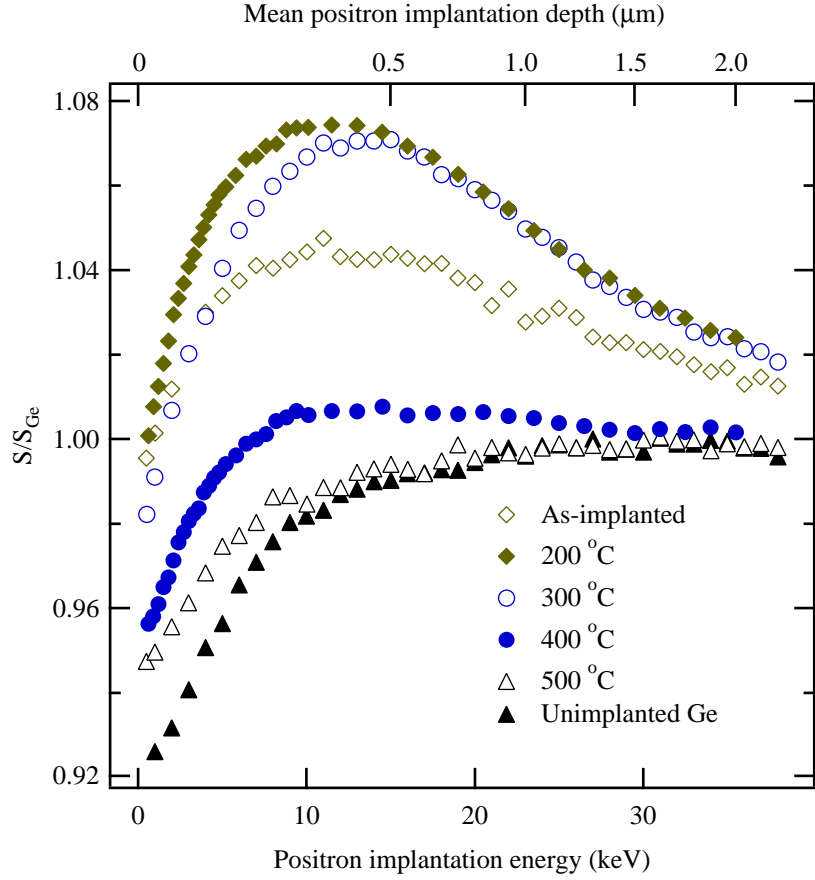


Figure 3.3: The low momentum  $S$  parameter measured at room temperature after 30 min anneal for the set 21-x with Si fluence  $1 \times 10^{12} \text{ cm}^{-2}$ . The data has been scaled to the parameters measured in bulk Ge with  $S_{Ge}=0.517$ .

The values of the  $S$  parameter at the peak and the corresponding lowest recorded  $W$  parameter value are shown in Fig. 3.4. In the samples with implantation fluence between  $10^{13} \text{ cm}^{-2}$  and  $10^{14} \text{ cm}^{-2}$  the annihilation parameters for both the Si and the Ge implanted layers are identical. No difference in defect evolution is observed between Si and Ge implantation when the estimated implantation damage was equal. In these samples the  $S$  parameter increases with annealing temperatures 200 - 400 °C while the  $W$  parameter is almost constant. The non-linear behavior of the  $S$  and the  $W$  parameters shows that the defect type changes in the annealing. For vacancy clusters in Si the increase in the  $W$  parameter with increasing cluster size becomes smaller even for small clusters as the cluster size increases [6]. This is in agreement with an increase in the open volume of the defect.

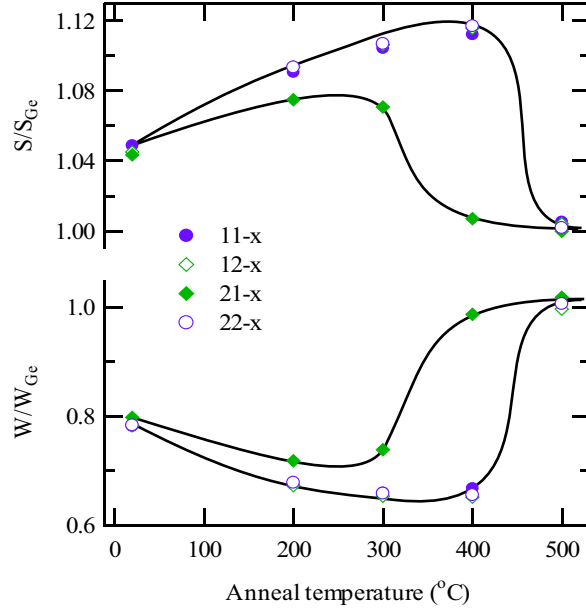


Figure 3.4: The  $S - W$ -plot of the parameter values corresponding to the top of the peak (bottom of the valley) of the  $S$  ( $W$ ) parameter curve. The data has been scaled to the parameters measured in bulk Ge with  $S_{\text{Ge}}=0.517$  and  $W_{\text{Ge}}=0.036$ .

The sample 21-2 annealed at 200 °C and implanted with a lower Si fluence  $1 \times 10^{12} \text{ cm}^{-2}$  also shows vacancy clustering. The defect type can be estimated from correlated changes of the  $S$  and  $W$  parameters. The measured  $S$  and  $W$  parameters cannot be obtained as a superposition of the bulk Ge parameters and the parameters of the samples annealed at 200 °C and implanted with a higher fluence. The observed  $S$  (or the  $W$ ) parameter of the sample 21-2 is too low indicating that the average size of the vacancies is smaller. After annealing at 300 °C the deviation of both the  $S$  and the  $W$  parameters from the bulk level reduces by 5 %. Linear changes of the parameters from the state corresponding to the bulk Ge show that the defect type is the same and the vacancy concentration is reduced by 5 % i.e. some recovery is already observed. After annealing at 500 °C both annihilation parameters in all the studied samples are indistinguishable from bulk Ge.

Figure 3.5 shows the measured  $S$  and  $W$  parameters in bulk Ge and samples 12-2 and 12-4 in the  $S$ - $W$ -plane for different positron implantation energies. The points corresponding to the bulk Ge sample fall on a line. This is typical when the annihilation fractions in two different positron states, the Ge surface and the bulk Ge, varies. The implanted samples, on the other

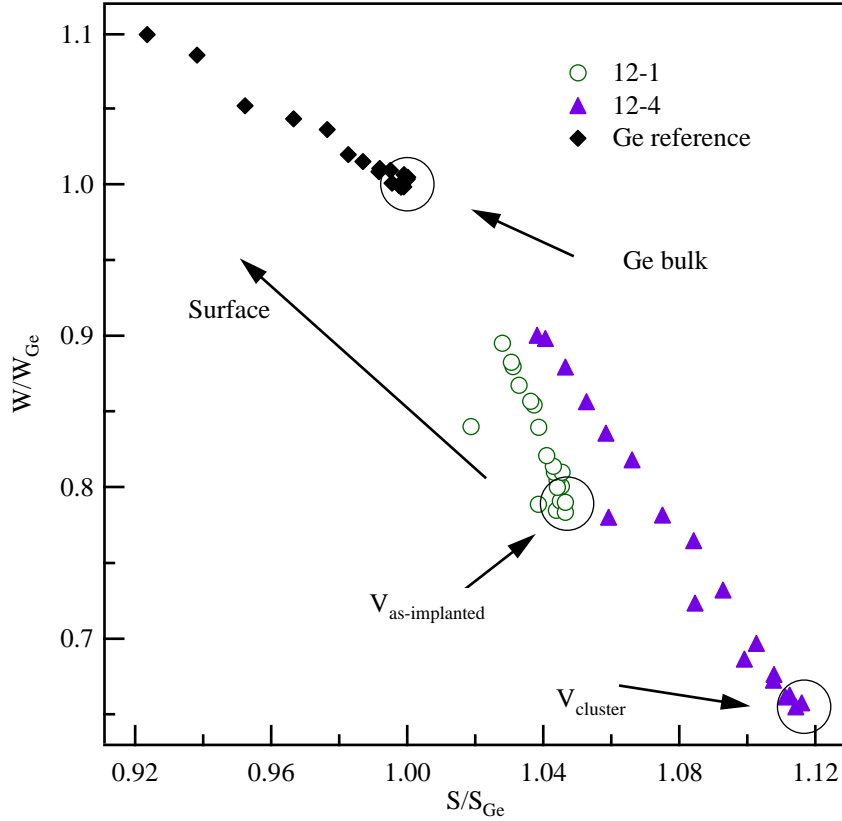


Figure 3.5: The  $S - W$ -plot of the parameter values corresponding to the top of the peak (bottom of the valley) of the  $S$  ( $W$ ) parameter curve. The data has been scaled to the parameters measured in bulk Ge with  $S_{\text{Ge}}=0.517$  and  $W_{\text{Ge}}=0.036$ .

hand, have all the points along two lines and the intersection is very sharp. The two lines show that there are three positron states in the samples; surface, defect and bulk Ge. At the positron implantation depth corresponding to the turning point all the positrons annihilate in defects. The saturated trapping into defects can be used to identify the defects. The 4.7 % increase in the  $S$  parameter is clearly larger than expected for a monovacancy where a 2-3 % increase in the  $S$  parameter would be expected. Typically a point defect of divacancy size in semiconductors has a  $S$  parameter value in the 1.04-1.06 range. At the same time there is a corresponding 22 % decrease in the  $W$  parameter. The annihilation parameters for a divacancy in Si have been determined as  $S = 1.052(3)$  and  $W = 0.78(2)$ , [14] which are close to the measured parameters. However, since RBS/channeling clearly shows that the

highest ion fluencies have amorphized the samples and considerable damage is seen already with ion fluencies in the  $10^{13} \text{ cm}^{-2}$  range it is likely that the measured annihilation parameters are characteristic for amorphous or highly disordered germanium. For the case of sample implanted with the lowest fluence the damage is not expected to be as high and the main positron trapping center could therefore be the divacancy.

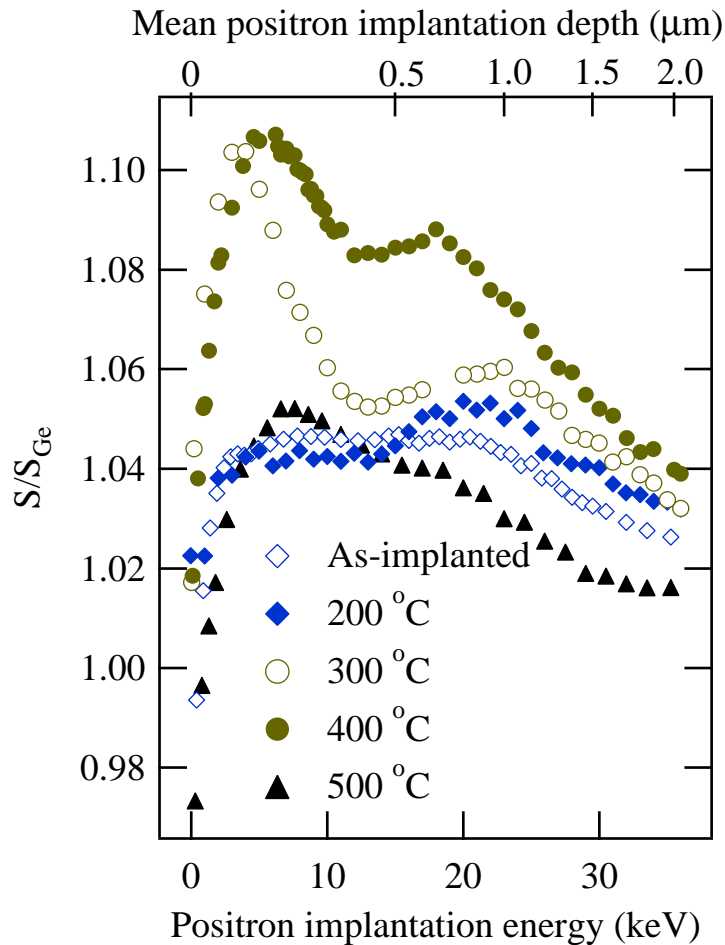


Figure 3.6: The low momentum  $S$  parameter measured at room temperature after 30 min anneal for the set 13-x with Si fluence  $4 \times 10^{14} \text{ cm}^{-2}$ . The data has been scaled to the parameters measured in bulk Ge with  $S_{\text{Ge}}=0.517$ .

Figures 3.6 and 3.7 show the annealing behavior of highest implantation fluencies for the Si and Ge implanted samples, respectively. As can be seen the behavior is quite different from the lower fluencies. RBS/C measurements of the Ge implanted sample showed complete amorphization, this is

also expected for the Si implanted case. Already at 200 °C a peak in the  $S$  parameter starts to develop at a depth of approximately 1  $\mu\text{m}$ . When the annealing temperature is increased to 300 °C a second peak near the surface appears in the silicon implanted sample. This peak continues to grow and reaches approximately the same  $S$  parameter value as the single peak observed in the samples implanted with a lower fluence. The peak at 1  $\mu\text{m}$  grows with increasing annealing temperature for both the silicon and germanium implantation, a slight shift towards the surface can also be seen. The height of the deeper peak is approximately  $1.08 \times S_B$ .

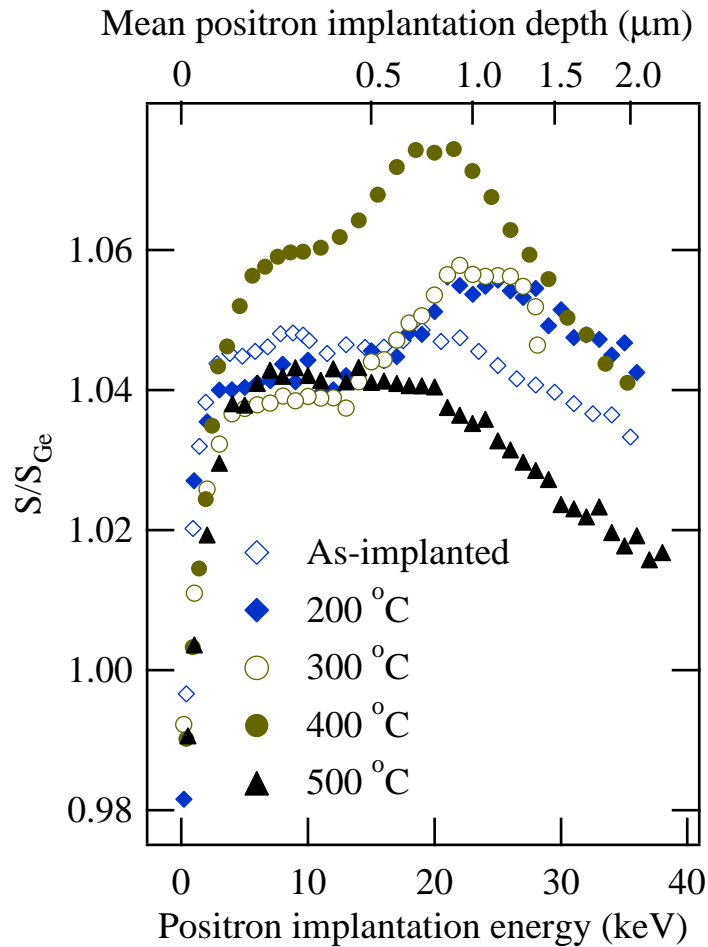


Figure 3.7: The low momentum  $S$  parameter measured at room temperature after 30 min anneal for the set 14-x with Ge fluence  $1 \times 10^{14} \text{ cm}^{-2}$ . The data has been scaled to the parameters measured in bulk Ge with  $S_{\text{Ge}}=0.517$ .

The annealing behavior in PAS measurements of the samples implanted with fluencies  $1 \times 10^{14} \text{ cm}^{-2}$  or higher clearly differ from the lower fluencies. This could be due to the zipper defect observed in RBS/channeling study, which could prohibit or slow down the agglomeration of vacancy defects into larger clusters.



# Chapter 4

## Conclusions

We have studied implantation damage in Si and Ge implanted Ge, with the ion fluence varying between  $1 \times 10^{12} \text{ cm}^{-2}$  and  $4 \times 10^{14} \text{ cm}^{-2}$ . Positron annihilation spectroscopy and Rutherford backscattering/channeling have been used for characterization of lattice damage, extended and point defects. In the as-implanted samples, channeling measurements show considerable lattice damage already at a fluence of  $1 \times 10^{13} \text{ cm}^{-2}$  and the fluence  $1 \times 10^{14} \text{ cm}^{-2}$  was enough to amorphize the crystal structure. Positron annihilation spectroscopy in the Doppler broadening mode give the annihilation parameters  $S=1.047$  and  $W=0.79$  independently of ion and fluence for the as implanted samples. The annihilation parameters indicate an average free volume approximately of divacancy size. In annealed layers channeling measurements show recovery of the damaged region beginning from the surface and vacancy clustering is detected by positrons. The cluster size depends on the fluence. Annealing at  $500 \text{ }^\circ\text{C}$  was enough to remove all the defects when the ion fluence was below  $4 \times 10^{14} \text{ cm}^{-2}$ .

The authors wish to acknowledge the contribution of the late Professor K. Saarinen for this work.

# Bibliography

- [1] M. L. Lee, E. A. Fitzgerald, M. T. Bulsara, M. T. Currie, and A. Lochtefeld, *J. Appl. Phys.* **97**, 011101 (2005).
- [2] R. Krause-Rehberg and H. S. Leipner, *Positron Annihilation in Semiconductors* (Springer, Berlin, 1999).
- [3] P. Moser, J. L. Pautrat, C. Corbel, and P. Hautojärvi, in *Positron annihilation*, edited by P. C. Jain, M. Singru and K. P. Gopinathan (World Scientific Publ. Co., Singapore, 1985), p. 733.
- [4] R. Krause-Rehberg, M. Brohl, H. S. Leipner, T. Drost, A. Polity, U. Beyer, and H. Alexander, *Phys. Rev. B* **47**, 13266 (1993).
- [5] K. Saarinen, P. Hautojärvi, and C. Corbel, in *Identification of Defects in Semiconductors*, edited by M. Stavola (Academic Press, New York, 1998), p. 209.
- [6] M. Hakala, M. J. Puska, and R. M. Nieminen, *Phys. Rev. B* **57**, 7621 (1998).
- [7] B. Nielsen, . W. Holland, T. C. Leung, and K. G. Lynn, *J. Appl. Phys.* **74**, 1636 (1993).
- [8] P. Ehrhart and H. Zillgen, *J. Appl. Phys.* **85**, 3503 (1999).
- [9] A. R. Peaker, V. P. Markevich, L. I. Murin, N. V. Abrosimov, and V. V. Litvinov, *Mater. Sci. Eng., B* **124-125**, 166 (2005).
- [10] V. P. Markevich, I. D. Hawkins, A. R. Peaker, K. V. Emtsev, V. V. Emtsev, V. V. Litvinov, L. I. Murin, and L. Dobaczewski, *Phys. Rev. B* **70**, 235213 (2004).
- [11] L. Csepregi, R. P. Küllen, J. W. Mayer, and T. W. Sigmon, *Solid State Commun.* **21**, 1019 (1977).

- [12] I. Suni, G. Göltz, M.-A. Nicolet, and S. S. Lau, *Thin Solid Films* **93**, 171 (1982).
- [13] A. Satta, E. Simoen, T. Clarysse, T. Janssens, A. Benedetti, and B. de Jaeger, *Appl. Phys. Lett.* **87**, 172109 (2005).
- [14] H. Kauppinen, C. Corbel, K. Skog, K. Saarinen, T. Laine, P. Hautojärvi, P. Desgardin, and E. Ntsoenzok, *Phys. Rev. B* **55**, 9598 (1997).